



HAL
open science

Forest aging limits future carbon sink in China

Yi Leng, Wei Li, Philippe Ciais, Minxuan Sun, Lei Zhu, Chao Yue, Jinfeng Chang, Yitong Yao, Yuan Zhang, Jiaxin Zhou, et al.

► **To cite this version:**

Yi Leng, Wei Li, Philippe Ciais, Minxuan Sun, Lei Zhu, et al.. Forest aging limits future carbon sink in China. *One Earth*, 2024, 7 (5), pp.822 - 834. 10.1016/j.oneear.2024.04.011 . hal-04581571

HAL Id: hal-04581571

<https://hal.science/hal-04581571>

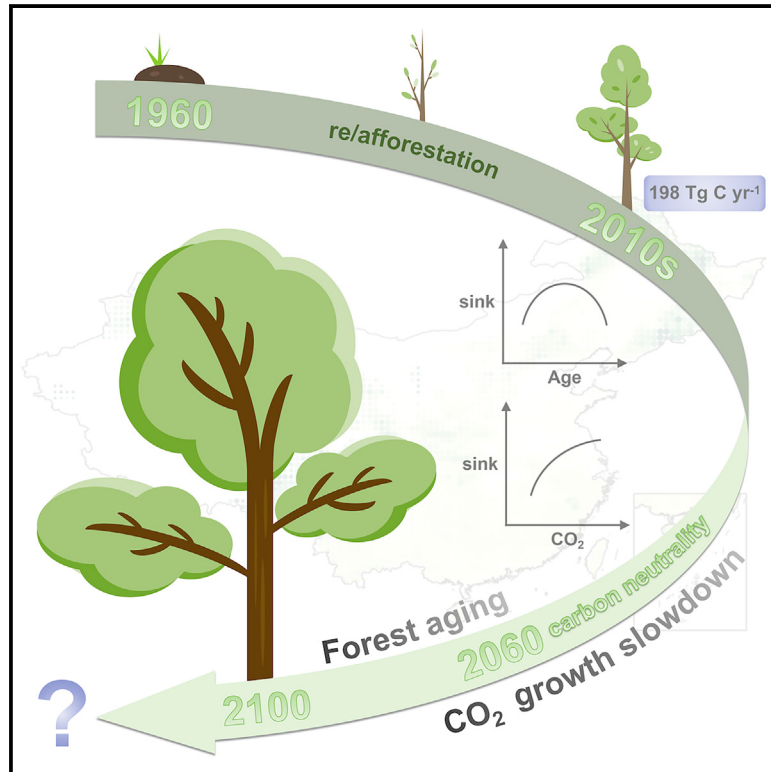
Submitted on 21 May 2024

HAL is a multi-disciplinary open access archive for the deposit and dissemination of scientific research documents, whether they are published or not. The documents may come from teaching and research institutions in France or abroad, or from public or private research centers.

L'archive ouverte pluridisciplinaire **HAL**, est destinée au dépôt et à la diffusion de documents scientifiques de niveau recherche, publiés ou non, émanant des établissements d'enseignement et de recherche français ou étrangers, des laboratoires publics ou privés.

Forest aging limits future carbon sink in China

Graphical abstract



Authors

Yi Leng, Wei Li, Philippe Ciais, ..., Xuhui Wang, Yi Xi, Shushi Peng

Correspondence

wli2019@tsinghua.edu.cn

In brief

Land-use and land-cover changes result in a complex forest age structure in China, raising challenges in estimating the forest carbon sink. Using a process-based ecosystem model with an explicit representation of forest age cohorts, we estimated the present-day forest carbon sink in China and found that the future carbon sink will be limited due to forest aging and the slowdown of atmospheric CO₂ growth. Our study emphasizes the importance of considering forest age dynamics in policy making to achieve the carbon neutrality goal.

Highlights

- A model with forest age dynamics was used to estimate carbon sink
- China's terrestrial carbon sink in the 2010s was estimated as $198 \pm 54 \text{ Tg C yr}^{-1}$
- Forest aging and the slowdown of atmospheric CO₂ growth limit future carbon sink



Article

Forest aging limits future carbon sink in China

Yi Leng,¹ Wei Li,^{1,2,9,*} Philippe Ciais,³ Minxuan Sun,¹ Lei Zhu,¹ Chao Yue,⁴ Jinfeng Chang,⁵ Yitong Yao,⁶ Yuan Zhang,⁷ Jiaxin Zhou,¹ Zhao Li,¹ Xuhui Wang,⁸ Yi Xi,⁸ and Shushi Peng⁸

¹Department of Earth System Science, Ministry of Education Key Laboratory for Earth System Modeling, Institute for Global Change Studies, Tsinghua University, Beijing 100084, China

²Ministry of Education Ecological Field Station for East Asian Migratory Birds, Department of Earth System Science, Tsinghua University, Beijing, China

³Laboratoire des Sciences du Climat et de l'Environnement LSCE, Orme de Merisiers, 91191 Gif-sur-Yvette, France

⁴State Key Laboratory of Soil Erosion and Dryland Farming on the Loess Plateau, Northwest A&F University, Yangling, Shaanxi 712100, China

⁵College of Environmental and Resource Sciences, Zhejiang University, Hangzhou, China

⁶Laboratoire des Sciences du Climat et de l'Environnement, LSCE/IPSU, CEA-CNRS-UVSQ, Université Paris-Saclay, 91191 Gif-sur-Yvette, France

⁷Key Laboratory of Alpine Ecology, Institute of Tibetan Plateau Research, Chinese Academy of Sciences, Beijing 100101, China

⁸Sino-French Institute of Earth System Sciences, College of Urban and Environmental Sciences, Peking University, Beijing, China

⁹Lead contact

*Correspondence: wli2019@tsinghua.edu.cn

<https://doi.org/10.1016/j.oneear.2024.04.011>

SCIENCE FOR SOCIETY Forest carbon sinks are vital in efforts to mitigate climate change, as they absorb a considerable amount of human-emitted carbon dioxide. In recent decades, large-scale ecological restoration projects such as the Three-North Shelter Forest Program, the Yangtze River and Zhujiang River Shelter Forest Projects, and the Grain for Green Program have helped China recover forest area following massive loss prior to the 1960s, growing its land-based carbon sink. Young forests are more productive than older, more mature forests, which makes them more effective at absorbing carbon dioxide. However, this means that as forests age, they become less effective at mitigating climate change. Forecasting ahead to the year 2100, the work presented in this article shows that forest aging and the slowdown of atmospheric CO₂ growth will reduce China's land-based carbon sink by up to 1.1 Tg of carbon per year. Considering the commitment to achieving carbon neutrality by 2060, China needs to recognize the limitations of forests as a climate mitigation tool and promote stringent emission reductions in other sectors.

SUMMARY

Forest age structure, shaped by past land-use and land-cover changes (LULCC), is pivotal for estimating ecosystem carbon sinks. China's extensive LULCC in recent decades has led to a complex forest age structure, but its impact on the carbon sink remains uncertain. Here, using a process-based ecosystem model with an explicit representation of forest age cohorts, we estimate China's terrestrial carbon sink as $198 \pm 54 \text{ TgC yr}^{-1}$ in the 2010s, mainly contributed by middle-aged forests. The existing forests in 2020 contribute most to the future total carbon sink, but its contribution will decrease significantly by $-1.1 \sim -0.35 \text{ TgC yr}^{-1}$ until 2100 due to forest aging and the slowdown of CO₂ concentration growth. Future re/afforestation will enhance carbon sink by increasing forest area and rejuvenating forest demography. Our study emphasizes the limited future carbon sink due to forest aging, implying that realizing China's carbon neutrality should not rely excessively on ecosystem carbon sink.

INTRODUCTION

Terrestrial carbon sinks, controlled by environmental and climate factors, and by direct anthropogenic activities^{1,2} provide a global mitigation of climate warming by absorbing about one-third of human-caused CO₂ emissions.^{3,4} Forest carbon sinks, a key component of the global land sink, originate from tree growth

after land-use and land-cover changes (LULCC) such as re/afforestation.⁵ Net primary productivity (NPP) is strongly influenced by variations in stand age and environmental conditions.⁶ Changes in environmental conditions, such as increasing atmospheric CO₂ concentrations, can stimulate photosynthesis and maintain old-growth forests as carbon sinks.^{7,8} However, the impact of regional climate change on forest sinks can vary, as



it can either enhance or reduce vegetation activity and affect phenological patterns.^{9–11}

In China, the forest area has changed dramatically over the past 60 years with a gradual recovery from a massive loss before the 1960s¹² to a rapid increase in recent decades, due to large-scale ecological restoration projects,^{13–15} such as the Three-North Shelter Forest Program, the Yangtze River and Zhujiang River Shelter Forest Projects, and the Grain for Green Program.¹⁶ The result of this history of forest land use is a complex pattern of forest age structure, dominated by young forests.^{17,18} Young forests have superior productivity, and the growth rate of aboveground biomass stocks in the tropical secondary forests is found much larger than that in old-growth forests.¹⁹ This can be attributed to the decline of NPP with forests aging, which is primarily driven by the decrease of gross primary productivity (GPP).²⁰ Therefore, ignoring age effects can lead to biased results in estimating China's forest carbon sink.

Previous studies have estimated China's terrestrial carbon sink through various approaches such as biomass and soil carbon inventories,^{21,22} upscaling of data from eddy covariance flux towers,^{23,24} ecosystem process models,^{25–27} and atmospheric inversions.^{28,29} While these studies have attributed the terrestrial ecosystem carbon sink in China mainly to forest area expansion, CO₂ fertilization, and climate change,^{13,30} the impact of forest age dynamics has not been explicitly quantified. Although empirical relationships have been established between forest age and growth based on observations, they mainly focus on specific species³¹ or specific locations.³² On the other hand, process-based dynamic global vegetation models (DGVMs) can simulate spatially explicit carbon, water, and energy cycle,³³ and the implementation of forest age cohorts provides a new capacity for accurately capturing the forest carbon dynamics induced by the temporal evolution of forest demography.^{5,34} However, the inaccurate representation of the LULCC history¹² and the lack of consideration for forest age dynamics in most DGVMs in the global carbon project²⁶ limit their ability to accurately simulate the terrestrial carbon sink in China. In China, natural disturbances such as forest diseases, pests, and wildfires are not very intense and have a relatively small impact³⁵ (Figure S1), with the current forest demography being more strongly determined by historical LULCC such as re/afforestation and by forest management driven by wood harvesting. Therefore, accurate LULCC input data are crucial for DGVMs to accurately simulate the forest age cohorts and estimate the contribution of the forest carbon sink to China's carbon neutrality target.³⁶

Here, we aim to estimate the present-day forest carbon sink in China by explicitly considering the forest age structure and further predict the contributions of different climatic and anthropogenic factors to future forest carbon sink. We use a DGVM (ORCHIDEE-MICT³⁷) with an explicit representation of forest age cohorts³⁴ to simulate the contemporary terrestrial carbon sink and the future forest carbon sequestration in China. New historical gross land-use change (LUC) information is aggregated from multiple sources including high-resolution remote sensing products,³⁸ inventory-based statistics,^{16,35,39–41} and historical land-use datasets⁴² (experimental procedures). Further, we calibrate the historical LUC and wood harvest data according to a 2010 forest age map, downscaled from provincial inventory data based on lidar-derived forest height and climate

Table 1. LULCC forcing data used in the three simulations during 1960–2019

Simulation	LUC	wood harvest
S _{def}	Default LUC maps based on LUH2 ⁴⁴	Proportionally allocated national wood harvest biomass ⁴⁰ based on the simulated aboveground biomass across grid cells
S _{area}	Area-adjusted LUC maps based on multiple remote sensing and inventory data	Same as S _{def}
S _{age}	Same as S _{area}	Backcasted wood harvest distribution according to the forest age map from Zhang et al. ¹⁷ and area-adjusted LUC maps

data¹⁷ (experimental procedures). By explicitly considering forest demography for the historical period, we find China's terrestrial carbon sink is 198 ± 54 Tg C yr⁻¹ in the 2010s. We have validated our results against multi-source datasets and found that the model performed well for most components of the ecosystem carbon fluxes and pools in China (experimental procedures, Note S1 and Figure S2). We predict the CO₂ removal potential of a forest-based climate mitigation solution until 2100 according to the China's Nationally Determined Contributions (NDCs).⁴³ Future carbon sink in the existing forests in 2020 in China will decrease due to forest aging and the slowdown of atmospheric CO₂ growth by the end of the century, implying that the removal of carbon dioxide cannot rely solely on ecosystem carbon sink to achieve China's "carbon neutrality" target.

RESULTS

Forest age maps in 2010

We chose the year 2010 for the comparison of forest ages as given by the national forest inventory¹⁶ and the gridded forest age map from Zhang et al.,¹⁷ since the latter is only available for this year. Current forests in China were mainly established from forest restoration after wood harvest or LUC such as afforestation. Therefore, accurate LULCC input data are key for the model to simulate the current forest age structure. As the Land-Use Harmonization (LUH2) dataset⁴⁴ (the default LUC map in S_{def}, Table 1) does not properly reconstruct the observed forest area expansion in recent decades in China (Figure S3), we adjusted the historical LUC maps from LUH2 based on multiple remote sensing and inventory data (experimental procedures, the map used in S_{area} and S_{age}). We further constrained the wood harvest based on the gridded forest age map from Zhang et al.¹⁷ (i.e., different wood harvest forcings between S_{area} and S_{age}). We thus performed three simulations (S_{def}, S_{area}, and S_{age}) with the same model configurations but different LUC and wood harvest forcing data (experimental procedures, Table 1). S_{age} with calibrated LUC and wood harvest data refers to the simulation with the best estimate of forest age in 2010.

We compared results from different simulations with the gridded forest age map¹⁷ and national forest inventory¹⁶ (Figure 1).

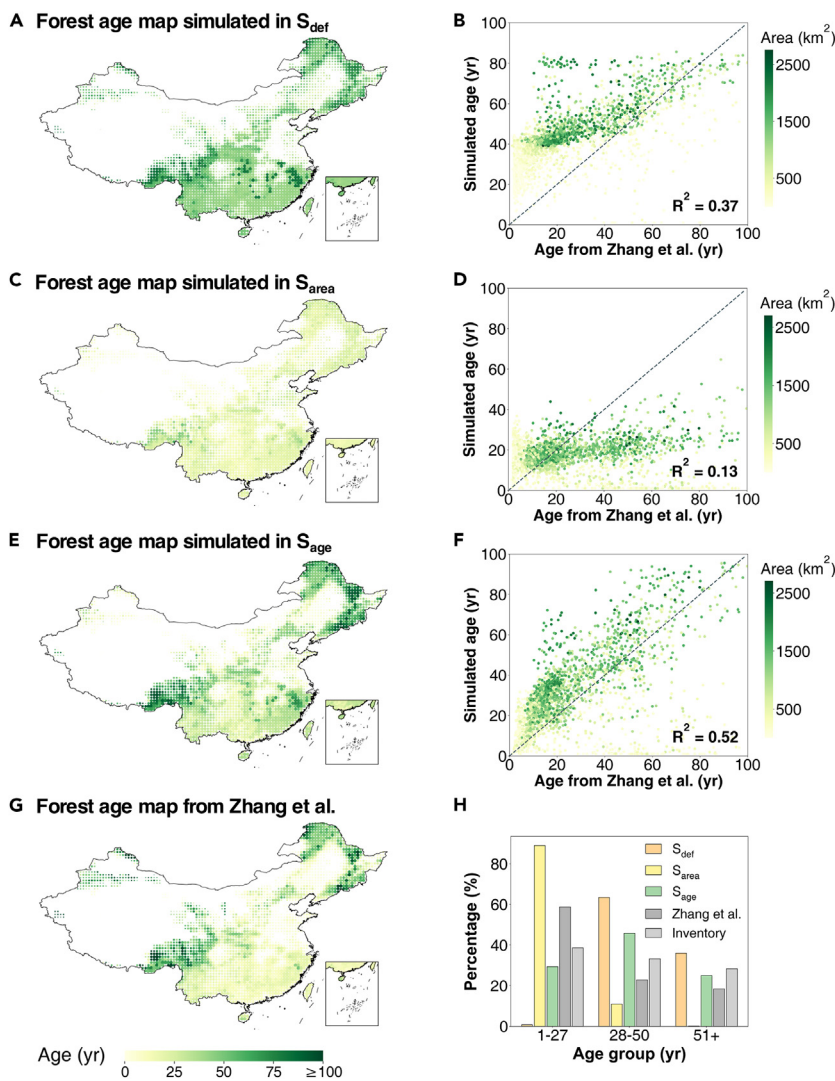


Figure 1. Comparison of model-simulated and observation-based forest ages in 2010

(A–F) Results for simulations using default LULCC map from the global carbon budget (S_{def} , A, B), adjusted LUC map and the default wood harvest data (S_{area} , C, D), and adjusted LUC map coupled with adjusted wood harvest data (S_{age} , E, F).

(G) The gridded forest age map from Zhang et al.¹⁷ The size of each dot in the forest age maps represents the relative size of forest area, and the color scale represents the average forest age in each $0.5^\circ \times 0.5^\circ$ grid cell. Note that only grid cells with both simulated and observed forest ages are shown. In (B), (D), and (F), the dashed line indicates the 1:1 ratio line.

(H) The comparison of forest area percentages in three age groups (1–27, 28–50, 51+ years) for the three simulated maps, the gridded age map from Zhang et al., and the forest inventory data.

of southwest and northeast China. In contrast, young forests are dominant in southern China where forests were clearcut before the 1980s, and extensive reforestation and afforestation have been conducted in recent decades.¹⁶ The southern provinces such as Guangxi and Yunnan are also the main wood production regions, with intensive wood harvest¹⁶ (Figure S4). However, the improved simulation with the S_{age} forcing underestimated forest age in small-scale areas (<500 km²) covered by old forests in northwest China, and slightly overestimates forest ages in southeast China (Figures 1E and 1G).

The area-weighted average forest age from S_{age} is 38.9 years, close to the average age reported previously (~42.6 years).¹⁷ The area percentage of forests younger than 50 years is 75% in S_{age} , consistent with the percentages of 81% calculated from the gridded forest age map from Zhang et al. and 72% from national inventories (Figure 1H). In contrast, the simulation using the default LULCC map strongly underestimates the percentage of forests younger than 27 years (1%, 59%, and 39%, respectively, for S_{def} , Zhang et al., and inventories, Figure 1H), indicating that mis-representing the LULCC history with less re/afforestation area in LUH2 severely underestimates the area of young forests.

Present-day land carbon sink and contributions

The net biome productivity (NBP) is used to account for the net carbon exchange between the biome surface and the atmosphere,⁶ and is the difference between net carbon absorption by vegetation and carbon release through soil respiration and disturbances. The terrestrial ecosystem carbon sink in China from the S_{age} simulation increased from 91 ± 48 Tg C yr⁻¹ (mean and interannual variability; positive values for land carbon sink) in the 1960s to 198 ± 54 Tg C yr⁻¹ in the 2010s with a significantly increasing trend of 1.69 Tg C yr⁻² ($p < 0.05$) over the period of 1960–2019 (Figure 2A; Table S1). The increasing terrestrial carbon sink is closely associated with the forest area

Gridded forest age map from Zhang et al.¹⁷ was generated by downscaling the provincial statistics of national forest inventory data into 1 km resolution, while the inventory data refer to statistical data at the national scale published by China's forestry department.¹⁶ The area percentages of different forest age groups at the national scale are not fully consistent between Zhang et al.¹⁷ and the inventory data (Figure 1H), likely because of some biases when downscaling the provincial data to gridded data in Zhang et al.¹⁷ The forest ages in 2010 are largely overestimated in S_{def} (Figures 1A and 1B) because the actual re/afforestation areas were not properly included in LUH2 which was used in S_{def} (Figure S3). After adjusting the LUC area (S_{area}), the simulated forest ages match Zhang et al.'s map in southern China but still underestimate the values in other regions (Figures 1C and 1G). With further constraints obtained from the gridded forest age map from Zhang et al. (S_{age} , experimental procedures), the simulation can generally reproduce inventory-based forest age structures (Figures 1E–1G).

Spatially, old forests are mainly concentrated in regions with less anthropogenic disturbance, such as the mountainous areas

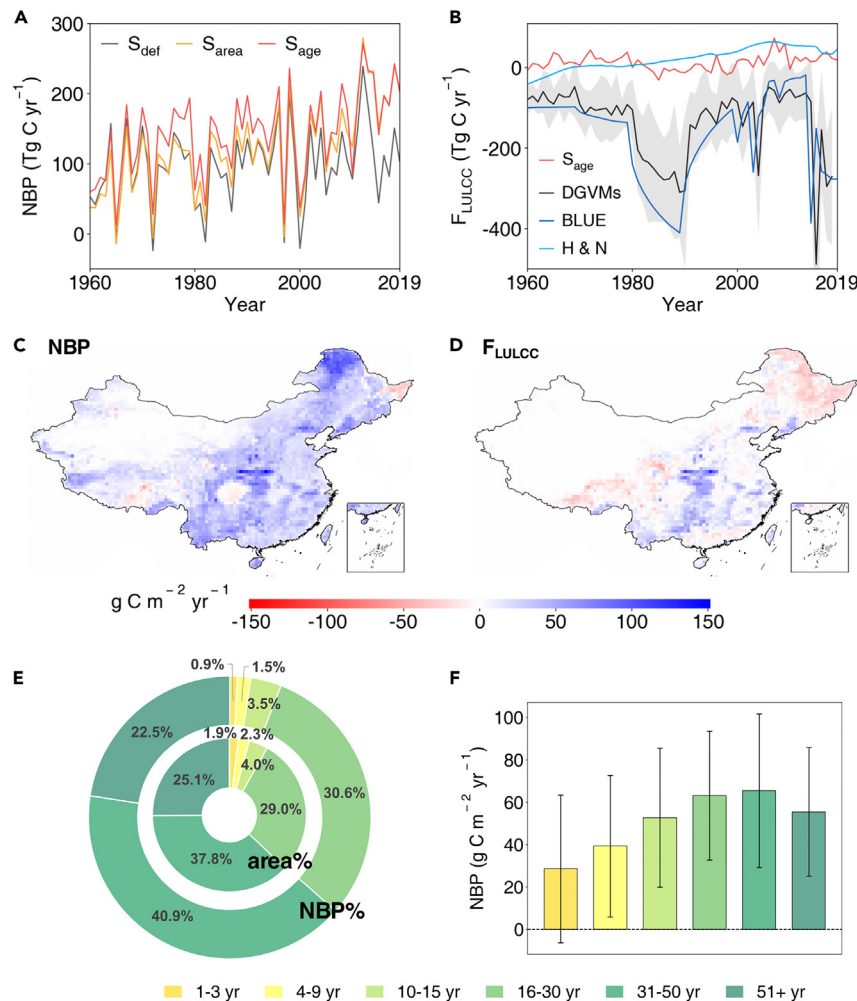


Figure 2. Temporal changes and spatial distribution of historical carbon fluxes and the contributions from different age cohorts

(A–D) Time series of (A) NBP in the three simulations using different LULCC forcing data (S_{def} , S_{area} and S_{age}) and (B) land-use and land-cover change flux (F_{LULCC}) in S_{age} and previous studies. The black line in (B) indicates the mean value of F_{LULCC} from 12 DGVMs from the global carbon budget, and the gray shading denotes the standard deviation. Maps of (C) NBP and (D) F_{LULCC} in S_{age} are averaged over 2010–2019. Positive values of NBP and F_{LULCC} indicate terrestrial carbon sinks, and negative values indicate terrestrial carbon sources. (E) Percentages of forest areas and cumulative NBP among different forest age cohorts and (F) their carbon sequestration rates during 2010–2019. The inner ring in (E) indicates the area percentages in 2010, while the outer ring indicates the percentages of cumulative NBP during 2010–2019. Error bars in (F) represent the standard deviation (spatial variation) of annual mean carbon sequestration rates during 2010–2019 across all grid cells.

expansion after 1950 (Figure S3). Temporal fluctuations in the terrestrial ecosystem NBP are mainly contributed by the non-forest ecosystems, probably due to its larger area in China¹⁶ (Figure S3), and these variations may be associated with variabilities of temperature and precipitation due to El Niño Southern Oscillation (ENSO) events.⁴⁵ Although NBP from S_{age} is similar to that from S_{area} ($203 \pm 45 \text{ Tg C yr}^{-1}$) in the 2010s (Table S1), the cumulative NBP during 1960~2019 from S_{age} is 8.5 Pg C, which is 1.3 Pg C higher than that from S_{area} (Figure S5). By contrast, S_{def} underestimates both NBP in the 2010s ($126 \pm 56 \text{ Tg C yr}^{-1}$) and cumulative NBP during 1960~2019 (5.8 Pg C) compared to the results from S_{age} (Table S1; Figure S5).

The carbon flux from LULCC (F_{LULCC} , positive values representing a land carbon sink) is inferred from factorial simulations (with and without LULCC) as in the global carbon budget²⁶ (experimental procedures). F_{LULCC} shows a carbon sink during 2010–2019 ($21 \pm 12 \text{ Tg C yr}^{-1}$, Figure 2B), which is contrary to the LULCC fluxes estimated from the DGVMs ensemble²⁶ and the BLUE bookkeeping model⁴⁶ (-171 ± 138 and $-162 \pm 145 \text{ Tg C yr}^{-1}$, respectively, Figure 2B). These models used LULCC forcing based on LUH2, which has an unrealistic and persistent forest loss over time in China (Figure S3). In contrast, another bookkeeping model used by Houghton and Nassikas (H&N)⁴⁰

used forest area from the Forest Resource Assessment⁴¹ and produced a carbon sink ($48 \pm 9 \text{ Tg C yr}^{-1}$) from the massive afforestation area in China over recent past decades. However, the F_{LULCC} obtained by H&N lacks interannual variability because their model does not account for climate and environmental effects on F_{LULCC} .⁴⁰

In S_{age} , most regions in China show a carbon sink during 2010~2019, especially in the Great Xing'an Mountains in northeast China, around the Qinling mountains and in southwest China (Figures 2C; S6).

The strong carbon sink in the Great Xing'an Mountains is driven by climate change rather than by LULCC, since this region is mainly covered by natural forests and has a small F_{LULCC} (Figures 2C and 2D). In contrast, the carbon sink around the Qinling mountains and in southwest China is mainly contributed by previous re/afforestation and forest management, as indicated by the spatial consistency between NBP and F_{LULCC} (Figures 2C and 2D). In fact, F_{LULCC} indicates a strong carbon sink for the whole of southern China. However, in the eastern Heilongjiang Province, F_{LULCC} is a carbon source (Figure 2D) consistent with the sign of NBP (Figure 2C). Ecosystem carbon losses, of relatively small magnitudes, are also found in other small regions such as the Sichuan Basin and a few areas in western China (Figure 2C). In contrast, regional carbon sinks are severely underestimated when the default LULCC forcing, with continuous forest loss over time, is used (Figures S3; S6).

We further analyze the contribution of different forest age cohorts in 2010 to the forest carbon sink during 2010~2019. Middle-aged (16- to 50-year-old) forests cover 66.8% of the total forest area in 2010 and contribute 71.7% of the cumulative forest ecosystem NBP over 2010–2019 (Figure 2E). Young forests (≤ 15 years) have the smallest area and NBP contribution (8.2% and 6.0%, respectively). The NBP contribution of the older

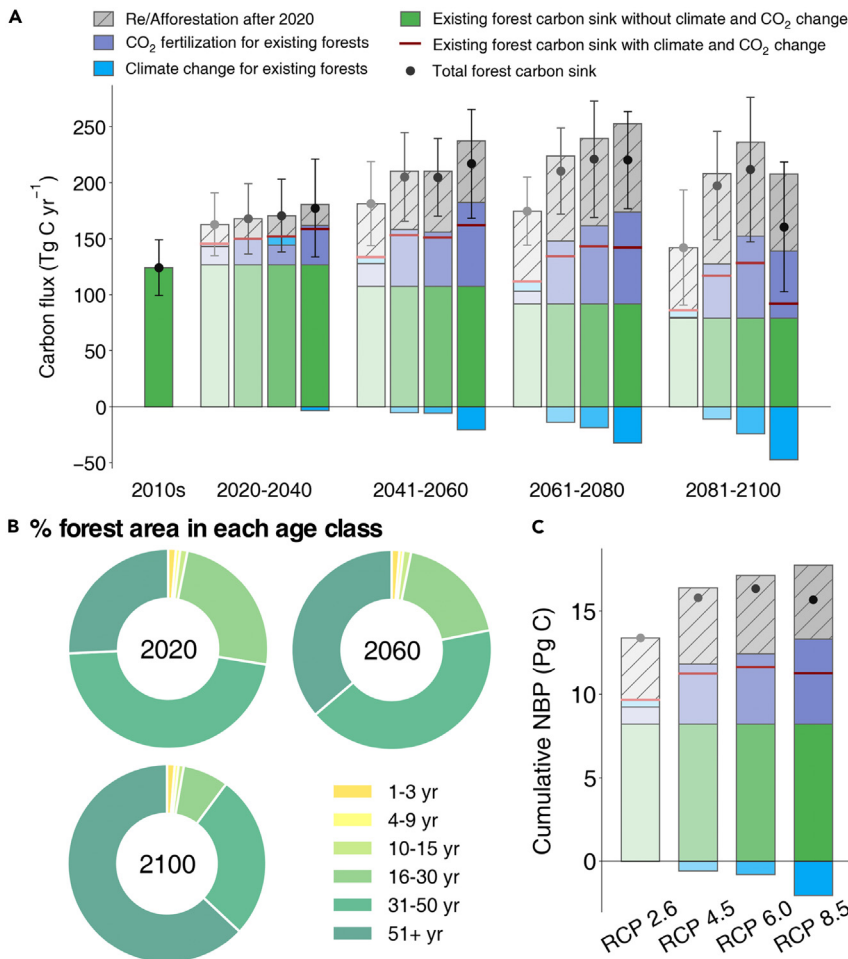


Figure 3. Composition of future forest carbon sink and forest age in China

(A) Contributions of different components to forest carbon sink in the 2010s from S_{age} and in each interval. Bars from left to right with deepening colors in each period represent results from the simulations under the RCP 2.6, RCP 4.5, RCP 6.0, and RCP 8.5 scenarios, respectively. The black dots and error bars indicate means and interannual variability of total forest carbon sink in each interval, and the red lines indicate the carbon sink contributed by existing forests in 2020. Black dot is the sum of all bars in a column, while red line is the sum of colored bars (i.e., purple, green, and blue bars) in a column. Future carbon fluxes shown here are the averaged values from two sensitivity tests using different LULCC maps (experimental procedures). Note that the contributions of CO₂ fertilization and climate change are only separated out for the existing forest ecosystem in 2020 (i.e., new afforestation after 2020 is not included).

(B) Forest age structure in 2020, 2060, and 2100. Total forest area for each forest age cohort is averaged over the four RCP scenarios and the two afforestation scenarios (experimental procedures).

(C) Cumulative NBP from 2020 to 2100. Positive values of carbon fluxes indicate terrestrial carbon sinks.

forests (22.4%) is also lower than their area fraction (25.0%). Therefore, the present-day forest carbon sink is mainly contributed by the middle-aged forests. Indeed, the carbon sequestration rate per unit area rises gradually from $29 \pm 35 \text{ g C m}^{-2} \text{ yr}^{-1}$ in the youngest forests (1–3 years old) to a peak of $66 \pm 36 \text{ g C m}^{-2} \text{ yr}^{-1}$ in the 31- to 50-year-old forests and then declines to $55 \pm 30 \text{ g C m}^{-2} \text{ yr}^{-1}$ in forests older than 50 years when the trees are becoming mature (Figure 2F).

Future forest carbon sink with dynamic forest demography

According to the Chinese NDCs,⁴³ forest coverage in China is planned to reach 24.1% by 2025 and 25% by 2030. We assume that forest cover will increase linearly to these targets in 2025 and 2030, and that later, during 2030–2060, the area growth rate will remain the same as that during 2025 and 2030 (experimental procedures). In 2060, the forest coverage achieved in this scenario is 30.5% (i.e., 0.69 Mkm^2 of forest increase from 2020 to 2060), close to the global forest coverage (30.7%).¹⁶ After 2060, we assume that forest area will remain constant until 2100 (i.e., no re/afforestation and deforestation). During 2021–2100, we assume a constant wood harvest rate identical to that in 2020 (experimental procedures). The average forest carbon sink during 2020–2100 ($160\text{--}206 \text{ Tg C yr}^{-1}$ under Represent-

tative Concentration Pathway 2.6, 4.5, 6.0, and 8.5; Table S2) is generally higher than in the 2010s ($124 \pm 25 \text{ Tg C yr}^{-1}$; Figure 3A). Specifically, China’s total forest carbon sink will increase after the 2010s to reach $181\text{--}217 \text{ Tg C yr}^{-1}$ during 2041–2060 (Figure 3A), but it will decline after 2060 under the Representative Concentration Pathway (RCP) 2.6 scenario and after 2080 under the RCP 4.5, 6.0, and 8.5 scenarios, reaching $142\text{--}212 \text{ Tg C yr}^{-1}$ during 2081–2100 (Figure 3A).

Negative impacts of climate change on the carbon sink of existing forests (i.e., forests established before 2020) are found under RCP 4.5, 6.0, and 8.5 (Figure 3A), but the overall impacts of future CO₂ fertilization and climate change are positive (Figure S7A). However, the carbon sink of “existing” forests established before 2020 will decrease from 145 to 159 Tg C yr^{-1} during 2020–2040 to $86\text{--}128 \text{ Tg C yr}^{-1}$ during 2081–2100 (Figure 3A), with a significant negative trend of $-1.1 \sim -0.35 \text{ Tg C yr}^{-1}$ ($p < 0.05$) over the period of 2020–2100 (Figure S8). The decrease is mainly caused by the aging of China’s forest demography under our assumption of a constant harvest rate. More than half of middle-aged (16- to 50-year-old) forests, with the highest carbon sequestration rate today, will shift to the oldest age cohort (Figure 3B). Forests in the oldest age cohorts will also become older, and their corresponding carbon sequestration rate will decline from $55 \pm 30 \text{ g C m}^{-2} \text{ yr}^{-1}$ in the 2010s to $36 \pm 15 \text{ g C m}^{-2} \text{ yr}^{-1}$ in the 2090s (Figure S9). As a result, age-related growth in “existing” forests will decrease by $\sim 37.6\%$ until 2100 (Figure 3A).

In the future afforestation scenarios, we assume that the future afforestation is first converted from marginal land and then from natural grassland and pasture. We use two methods to define

marginal land: one based on model-simulated crop yields and the other based on the marginal land map given by Campbell et al.⁴⁷ Contributions of newly established forests in future afforestation programs to the land carbon sink will gradually increase over the next 40–50 years but this trend will be stable or even decrease after the 2060s (Figures 3A; S10C). Specifically, the carbon sink of future newly established forests is projected to increase from 10 to 11 Tg C yr⁻¹ in the 2020s to 63–78 Tg C yr⁻¹ in the 2060s due to the expansion in area of young forests with a higher carbon sequestration rate. By the 2090s, as those forests become mature, it will decrease to 55–84 Tg C yr⁻¹ (Figure S10C).

The cumulative forest ecosystem NBP for 2020–2100 with new forest expansion under various climatic conditions ranges from 13.4 to 16.4 Pg C (Figure 3C). It is 0.3–0.8 Pg C higher during 2021–2060 than during 2061–2100 under RCP 2.6 and RCP 8.5, but 0.7–1.2 Pg C lower under RCP 4.5 and RCP 6.0 (Figure S11). The cumulative carbon sequestration of existing forests is 9.8–11.6 Pg C (71.2%–72.3% of the total) while that of new afforestation is 3.7–4.7 Pg C (27.7%–28.8%) (Figure 3C). Most of the cumulative carbon sink in the existing forests originates from age-related growth (8.2 Pg C; experimental procedures). For these existing forests, CO₂ fertilization contributes 1.0–5.1 Pg C under various RCP scenarios. Climate change induces a small increase in the forest carbon sink (0.4 Pg C) under RCP 2.6 but a decrease under RCP 4.5, 6.0, and 8.5 (–2.1 ~ –0.6 Pg C, Figure 3C). In addition, cumulative NBP in the afforestation scenario where new forests are preferentially created from low-yield croplands is 0.6–0.9 Pg C lower than that if new forests are created on abandoned agricultural land (experimental procedures and Figure S11). This difference arises because most low-yield croplands are located in northwestern China with less favorable growing conditions, such as water stress and soil degradation (Figure S12). Note that areas of cropland abandonment only account for 20.9% of the future total afforestation area, with the remainder coming from areas of natural grassland and pasture (experimental procedures and Figure S12).

DISCUSSION

In this study, by explicitly considering forest demography caused by previous LULCC, we estimate China's terrestrial carbon sink during 2010–2019 to be 198 ± 54 Tg C yr⁻¹ (Figure 2A). Our result is within the reported range of 170–350 Tg C yr⁻¹ estimated by previous studies using various methodologies.⁴⁸ Our simulation using the default LULCC maps largely overestimates forest age (Figure 1B) and thus underestimates the carbon sink (Figure 2A), highlighting the importance of forest age structure on the land sink. A recent study¹² also reconstructed China's historical LULCC maps based on inventory data and high-resolution satellite images but did not explicitly present the effect of forest demography on the terrestrial ecosystem carbon sink. Their estimated China's terrestrial carbon sink during 2010–2019 is ~41% larger than our result at 280 ± 23 Tg C yr⁻¹. The difference is probably because they took nitrogen deposition, fertilization, and irrigation into account,¹² which may lead to an increased forest carbon sink, but these processes were not included in our model.

By explicitly representing forest age dynamics, we find that the middle-aged forests are the major contributor to the present-day

forest carbon sink due to their larger area and the higher carbon sequestration rate (Figures 2E and 2F). GPP is correlated with leaf area index (LAI), thus GPP increases rapidly before middle age and then decreases until maturity.⁴⁹ The age-driven decline in carbon sequestration capacity can be attributed to the decline in NPP,²⁰ which is caused by the smaller difference between GPP and autotrophic respiration (R_a, Figure S13A). The peak age for forest NPP varies from 30 to 55 years old in China according to different vegetation types and climate factors,⁵⁰ which is consistent with our model-simulated NPP peak (~30 years, Figure S13B). As litter production and soil organic carbon will increase with forest growth,^{51,52} the carbon emission from their decomposition (i.e., heterotrophic respiration, R_h) will increase steadily with age (Figure S13B). Considering the relatively small impacts of deforestation flux and wildfire emissions (Figure S13C), the variation in NBP is mainly driven by the balance between carbon input from NPP and carbon output from R_h (Figures S13B and S13C). The decreasing forest ecosystem carbon sink in old forests simulated by our model is consistent with the previous eddy covariance observations.²³

After considering the forest age classes, new re/afforestation, and future climate and CO₂ changes (experimental procedures), we find that China's forest ecosystem carbon sink will increase to 181–217 Tg C yr⁻¹ during 2041–2060 and then slightly decrease to 142–212 Tg C yr⁻¹ during 2081–2100 (Figure 3A). Our projected cumulative forest carbon sink of 6.8–8.0 Pg C during 2021–2060 (Figure S11) is lower than previous estimates for a similar period (8.89–13.92 Pg C for 2010–2050),^{53,54} partly because these studies neglected the impacts of wood harvest on forest age dynamics.

The existing forests contribute most to future total carbon sink, but this carbon sink in existing forests will decrease by –1.1 ~ –0.35 Tg C yr⁻¹ until 2100, after considering forest aging, climate change, and CO₂ increase (Figures 3A, 3B; S8). Although old-growth forests could still serve as a carbon sink due to gap-scale mortality events, CO₂ fertilization, and nitrogen deposition,^{8,55} this effect is highly uncertain and will decline with the slowing of atmospheric CO₂ growth under future climate mitigation scenarios, and old-growth forests will be exposed to disturbances that may cause large carbon losses. Continuing afforestation in the future is one way to maintain the area of young forest with its high carbon sequestration rates and potential, but it would be challenging. Large-scale surveys have shown that forestation may result in the loss of soil organic carbon (SOC) in some places, but the overall impact is SOC gain after afforestation in northern China.⁵⁶ In the model, SOC indeed decreases with afforestation, but this carbon loss can be completely offset by the end of the century by the faster growth in biomass carbon (Figure S14). Besides, afforesting grassland may lead to a decrease in SOC,⁵⁷ which could partly explain the decline of soil carbon storage in southern China (Figures S12B, S12E; S15). Therefore, afforestation in carbon-rich soils needs to be carefully designed and evaluated. Our projected forest area increase (0.69 Mkm² during 2020–2060) is about 82% of the forest area increase during 1981–2018 (0.84 Mkm²; Table S3). Our estimate is slightly larger than the available reforestation area estimated from the areas of suitable land and sloping and degraded farmland (0.58 Mkm²),⁵⁸ but it is smaller than the area of moderately and highly suitable forest habitat

land defined by the existing forest distribution and environmental factors such as soil type and aridity index (0.87 Mkm^2).⁵⁹ In fact, suitable land for afforestation is limited in China due to the large area of arid and semi-arid zones where trees cannot survive,⁶⁰ the required arable area for food security, and rapid urbanization.⁶¹ Future forestation may also have negative effects on biodiversity and ecosystem services in natural non-forest ecosystems,^{62,63} especially in grasslands, which could potentially contribute 18.5%–78.3% of the future forestation areas.⁶⁴ Therefore, future afforestation needs to maintain a balance between providing carbon sink and protecting other ecosystem services from non-forest vegetation. In contrast to continuing afforestation, proper forest management, such as thinning, selective logging, fertilization, and irrigation, may help to increase the future forest carbon sink more easily.^{36,65}

Although the overall contribution of forest ecosystems to the land carbon sink increases due to forest area expansion and CO_2 fertilization, the terrestrial carbon sink decreases during 2020–2100 in our simulation, as non-forest ecosystems (i.e., cropland, natural grassland, and pasture) turn from a carbon sink in the 2010s (74 Tg C yr^{-1}) to a carbon source ($-33 \sim -17 \text{ Tg C yr}^{-1}$) under the RCP 2.6, RCP 4.5, RCP 6.0, and RCP 8.5 scenarios; [Figure S10B](#); [Table S2](#)). Non-forest carbon loss is mainly contributed by natural grassland in the southwestern Tibetan Plateau ([Figure S16](#)), because, in our model, future warming accelerates permafrost thawing and microbial decomposition, leading to a greater amount of carbon losses to the atmosphere⁶⁶ ([Figure S7B](#)). Our estimate of the terrestrial carbon sink in the 2050s ($152\text{--}237 \text{ Tg C yr}^{-1}$, [Table S4](#)) is at the low end of the range of $0.15\text{--}0.52 \text{ Pg C yr}^{-1}$ obtained from a literature review.³⁶ In comparison, China's fossil carbon emissions in 2050 are projected to be $0.52\text{--}0.63 \text{ Pg C yr}^{-1}$ under the 1.5°C warming scenario and $2.78\text{--}5.40 \text{ Pg C yr}^{-1}$ under a “no policy” scenario.⁶⁷ Therefore, our projected terrestrial ecosystem carbon sink, despite being lower than previously expected, could still play an important role in offsetting part of the future fossil fuel emissions (24.1%–30.6% and 4.1%–8.3% of total emissions under the two scenarios, respectively).

To model the wood harvest, we specify that a part of above-ground biomass goes into litter, while the rest goes into wood product pools with 10- and 100-year turnover times (experimental procedures). Wood products are temporary carbon storage pools, and the stored carbon will eventually be released into the atmosphere after the wood product life cycle. In the terrestrial NBP calculation, we do not account for the delayed carbon emission from these wood product pools and thus may overestimate the NBP. Using forest-type specific coefficients for transferring harvested aboveground biomass into the wood product pools⁶⁸ ([Table S5](#)), the delayed carbon emissions from the decay of wood product pools are estimated at $17\text{--}28 \text{ Tg C yr}^{-1}$ during 1960–2100 (a cumulative emission of $3.1\text{--}3.2 \text{ Pg C}$, [Figure S17](#)). Consequently, the terrestrial carbon sink would decrease to $177 \pm 53 \text{ Tg C yr}^{-1}$ in the 2010s ([Figure 2A](#); [Figure S17](#)) if these delayed emissions are taken into account. Recent studies have suggested that using woody material in construction can make it a long-term carbon storage pool, and thus it can serve as a viable solution for future climate mitigation.⁶⁹ Harvest intensity would also adapt dynamically in accordance with the engineered wood demand, and the tradeoff between wood harvest emis-

sions and forest-regrowth sequestration is more complicated in reality⁷⁰ than the simple setting in the model.

Our study quantifies the importance of forest age dynamics on the carbon sink of China but has some uncertainties due to lack of accurate forcing data, model structure, and processes missing from the model. For example, there is no long-term, spatially explicit wood harvest data available, precluding our model from accurately reproducing the spatial variations of wood harvest and regrowth ([Note S2](#)). In the model, the biomass thresholds that delineate different age cohorts in each grid cell are constant over time,³⁴ which ignores the impacts of climate change and increasing CO_2 on the biomass boundaries between different cohorts ([Note S3](#)). Despite these fixed thresholds, the increase, peak, and subsequent decline of carbon sequestration rates with increasing forest age ([Figure 2F](#)) are in line with the trends in boreal and temperate forests given in a compilation of observations.⁷¹ However, age-related productivity may vary considerably across various species,³¹ and we did not further calibrate the biomass-age curve at the species level due to the lack of large-scale observations. Forest disturbances such as extreme drought, windstorms, and insect outbreaks may also cause tree mortality and regeneration and lead to changes in forest age structure,^{72–74} but these processes are not explicitly represented in our current model version ([Note S3](#)). For the CO_2 fertilization effect, we verified that the simulated NPP can generally reproduce the observed response of NPP to elevated CO_2 in four Free-Air CO_2 Enrichment (FACE) experiments⁷⁵ and the simulated values are generally within the range of synthesized experiment-based results⁷⁶ (experimental procedures, [Note S4](#), [Figure S18](#); [Table S6](#)). Nitrogen deposition was found to be an important factor driving the net ecosystem productivity in China's forests,²³ but unfortunately the model version used here did not incorporate nutrient fertilization and limitation ([Note S3](#)). In particular, limitations due to phosphorus, the export of nutrients by harvest, and forest fertilization were not considered ([Note S3](#)).

Because of the large population and the short transition time from carbon peaking (2030) to carbon neutrality (2060),⁷⁷ the achievement of China's “carbon neutrality” target is challenging, but it would be a significant contribution to the global climate mitigation. Our model-based results indicate that China's terrestrial ecosystems can still function as an important carbon sink in the near future, but the carbon sequestration rate will decrease due to forest aging and the slowdown of CO_2 concentration growth. In addition, future extreme weather events may cause tree mortality and the subsequent recovery, and these changes in forest age classes will further influence the carbon sink.⁷⁸ Therefore, it is necessary to incorporate age classes into more DGVMs or Earth System Models to accurately predict future ecosystem carbon dynamics. Considering the vast area and low quality of young and middle-aged natural forests in China,⁷⁹ improving natural forest quality through forest management would help enhance forest carbon sink in addition to re/afforestation. Although proper forest management may help adjust forest age structure and increase forest carbon sink, its effect could be limited. Therefore, the carbon dioxide removal required to realize China's “carbon neutrality” target and maintain it for the long term cannot persistently rely on the ecosystem carbon sink: it will also need stringent emission reductions in other sectors. Our analysis demonstrates

the importance of forest age dynamics to the carbon sink, which can be applicable for both tropical countries with extensive deforestation and potential reforestation^{80,81} and to countries in Europe and North America with intensive forest managements.^{82–84} After carbon neutrality is reached, global temperature will not be stabilized immediately because warming may rise further as the planetary state moving toward equilibrium.⁸⁵ In this case, maintaining the carbon sink in mature forests through management will become more important to help stop further global warming by removing atmospheric CO₂.

EXPERIMENTAL PROCEDURES

Resource availability

Lead contact

Further information and requests for resources should be directed to and will be fulfilled by the lead contact, Wei Li (wli2019@tsinghua.edu.cn).

Materials availability

This study did not generate new unique materials.

Data and code availability

This paper does not report original code.

All data that support the main findings in this study are available via figshare at https://figshare.com/articles/dataset/Limited_future_carbon_sink_in_China_as_forests_become_mature/24872973.

Adjusting historical LULCC maps for S_{area}

We reconstructed the LUC maps for 1700 to 2020 by integrating multiple data sources including remote sensing products, forest inventory reports, and a historical land-use database. Specifically, we used (1) 30-m satellite-based China's Land-Use/Cover Dataset (CLUD) for the year 2015,³⁸ (2) forest areas and temporal changes at the provincial scale derived from the second to the ninth national forest inventory data covering the period 1977–2018,^{16,86} (3) forest area in each province for each 50-year interval from 1700 to 1949,³⁹ (4) national forest area data for the year 2020 from the Global Forest Resources Assessment (FRA) report,⁴¹ (5) national total forest area from 1700 to 1980 compiled by H&N,⁴⁰ (6) inventory-based cropland areas in 2015 from China Statistical Yearbook,³⁵ and (7) annual maps of cropland and pasture at 5' × 5' resolution from the History Database of the Global Environment (HYDE version 3.2).⁴² It should be noted that from 1994 the threshold of canopy cover used to define a forest changed from 30% to 20% in the inventory data in China. We thus calibrated forest area before 1994 according to an experimental conversion formula⁸⁷ (Table S3).

Following the backward method (BM3) proposed by Peng et al.,⁸⁸ we adopted the satellite-based, CLUD land-cover map for 2015³⁸ as the base map (Figure S19). First, the ice and water fraction from CLUD and the urban and bare ground fraction from HYDE3.2⁴² were excluded from land-use transitions. We then adjusted the gridded forest area proportionally in each province in CLUD³⁸ to match the provincial total forest area from the national forest inventory data.¹⁶ The national forest inventory data are updated at least every 5 years, and for the in-between years the forest area was determined by linear interpolation. For the period before 1980 when the national forest inventory data were not available, we calculated interannual change of national total forest area from H&N,⁴⁰ and then allocated the national total change into the provincial- and grid-level data based on the proportion of forest area in each province³⁹ and each grid cell.³⁸ For the period after 2015, we increased the forest area linearly to the national total forest area reported in the FRA report.⁴¹

Because the cropland areas in 2015 from CLUD³⁸ do not fully match those from HYDE3.2,⁴² we allocated the inventory-based cropland areas in 2015 from the China Statistical Yearbook³⁵ preferentially to the overlapping cropland area between CLUD and HYDE3.2, with the remaining cropland area then allocated proportionally to the non-overlapping cropland grid cells from both maps. The annual changes in cropland areas from HYDE3.2⁴² were further used to update the annual cropland maps. Pasture area was also derived directly from HYDE3.2,⁴² with the remaining fraction in each grid cell assigned to natural grass. The allocation sequence is therefore: forest, cropland, pasture, and natural grass. Note that the total fraction of these land-

use types is constrained by the maximum vegetation fraction in a given grid cell, and the extra area is allocated proportionally to other grid cells with the same land-use type.

The allocation processes were conducted at the resolution of 5 arcmin, the same data resolution as HYDE3.2.⁴² When aggregating into the model resolution of 0.5° × 0.5°, the gross land-transitions were also recorded by accounting for sub-grid bidirectional transitions between two land-use types in each 0.5° × 0.5° grid cell.³⁴

LUC and wood harvest constrained by the observed forest age map for S_{age}

Both re/afforestation after LUC and regrowth after wood harvest and natural disturbance can establish new seedlings and modify forest age structure. Afforestation refers to the establishment of forests in areas where there were no forests previously, while reforestation refers to replanting or regrowth of forests in areas that have experienced forest loss. Note here we excluded regrowth after wood harvest from reforestation and considered it as a separate type. As the intensity and coverage area of natural disturbances are relatively small in China³⁵ (Figure S1), the influence of natural disturbances on forest demography was not explicitly considered in the simulations (Note S3). Therefore, we adjusted LUC and wood harvest to match the gridded forest age map for 2010.¹⁷ This reference forest age map was generated by downscaling the provincial stand age information to 1-km resolution using an observed climate dataset, a vegetation map, and a lidar-derived tree-height map.¹⁷ For forest grid cells without forest age information, we searched the nearest grid cells, which had at least 10 data records and took the average age. As the forest carbon sink increases rapidly with age during the early growth stage and tends to stabilize once the forest is approximately 50 years old,⁸⁹ six age cohorts with intervals of 1–3, 4–9, 10–15, 16–30, 31–50, and ≥ 51 years were set up in the model.³⁴ We did not further divide the oldest class (≥ 51 years) to more classes, because it is expected to have minor impacts on the total carbon sink, and our study focused on the forest area expansion that mainly occurred in the past 50 years.¹² To align with these six age cohorts, we converted the gridded forest age map to the fraction of each cohort in each 0.5° × 0.5° grid cell in 2010. We further backcasted the corresponding forest establishment periods that resulted in the current forest age structure (Figure S20). For example, if there is 20% of land covered with the first age cohort (1–3 years) in a given grid cell, it means that at least 20% of new forests were established through re/afforestation after LUC or regrowth after wood harvest during 2007–2009 (Figure S20). If the re/afforestation fraction based on the reconstructed LUC maps is smaller than that estimated from the forest age map, the remaining part is supplemented by wood harvest. If it is larger, no adjustment is made. Note that the oldest age cohort in the model is ≥ 51 years, and forest establishment before 1960 could not influence the simulated forest cohorts in 2010, so this allocation method was only applied for the period 1960–2009. For wood harvest before 1960 and after 2009, we used annual wood harvest biomass data from Houghton & Nassikas.⁴⁰ Wood harvest biomass was allocated in proportion to the simulated aboveground biomass in the previous year across grid cells and then converted to area fraction in each grid cell.

Future afforestation scenarios

In the Chinese NDCs, the targeted forest coverage is 24.1% by 2025 and 25% by 2030, i.e., an afforestation area of 0.08 and 0.16 M km² since 2020. We thus linearly increased forest area to the targets for the period of 2020–2025 and 2025–2030 and kept the rate of increase for 2025–2030 constant until 2060. Since we assume China's forest coverage will reach the global average (30.7%¹⁶) by 2060 (30.5%, afforestation area = 0.69 M km² since 2020), we kept the LUC maps constant after 2060. We assumed several guidelines for future forestation scenarios: (1) conservation of primary and old forests, (2) forest expansion mainly in grid cells with existing forests, (3) re-plantation after wood harvest. Following the “Grain for Green” policy in China, forest area increase preferentially comes from cropland. To ensure food security and to maintain the cropland area above the “red line of 120 million ha (=1.8 billion mu) of arable land” set by the government, new forests were first converted from marginal cropland. Here, we used two methods to define marginal cropland. The first is based on model-simulated crop yields, with cropland being converted to forest in sequence from the lowest to higher yields until the remaining cropland area reached 120 million ha. The second method is based

on the marginal land map given by Campbell et al.,⁴⁷ representing abandoned agricultural lands. After all the marginal land from Campbell et al. was converted into forest, other cropland with the lowest simulated yields was converted sequentially until the “red line” was reached (in the same way as for the first method). When all marginal land from both methods was used up, there is still an area gap to the forest increase target. Forest area was then expanded on natural grassland and then, finally, on pasture if no further natural grass was available. In this final step, the forest expansion area is proportional to the existing forest area in each grid cell. For wood harvest, we kept the harvested amount constant at the 2020 value throughout the future period.

Model calibration and evaluation

We used ORCHIDEE-MICT³⁷ with explicit representations of gross LUC, wood harvest, and forest age dynamics³⁴ for our simulations. The PFT-specific parameters related to vegetation dynamics are prescribed based on field and satellite observations or empirical data, and the simulated diurnal and seasonal carbon and surface energy fluxes can generally reproduce the observations at FluxNet sites.⁹⁰ This model is capable of reflecting the influence of climatic changes on ecosystem carbon cycle, such as increased heterotrophic and maintenance respiration due to temperature warming.⁹⁰ In the previous version of ORCHIDEE-MICT (v8.4.1), several new processes and parameterizations were incorporated into the model for high latitudes, and the simulated water budget, air-to-soil temperature, and gross and net CO₂ fluxes for the terrestrial Northern Hemisphere (>30°N) have been extensively validated against satellite observations, *in situ* measurements, inventories, and gridded observation-based datasets.³⁷ A more advanced version of ORCHIDEE-MICT (v8.4.2) was developed to account for gross LUC and wood harvest with dynamic sub-grid age cohorts,³⁴ which can better simulate carbon dynamics caused by LULCC both on the site and global scales.^{34,68} Significant aging processes such as maintenance respiration increase and below-ground allocation decrease with forest aging were implemented in the model.³⁴ Recently, this model version was applied to demonstrate the importance of gross LUC in controlling the interannual variability of the land carbon cycle, but validation against aboveground biomass (AGB) observations showed underestimation in the northeast of Eurasia.⁹¹

Specifically for China, a mismatch of national total AGB was also found in our initial simulations (Figure S21A) due to the inappropriate parameterizations or missing processes in the model⁹¹ (Note S3). The simulated AGB was lower than satellite-based AGB observations (Figure S21B), especially for boreal forests (Figure S22). We thus calibrated two critical parameters for AGB in the model, i.e., LAI and maximum carboxylation rate (V_{cmax}), based on local field measurements⁹² (Table S7). After calibration, the simulated AGB generally matches the observed total AGB (Figure S21A), and the bias is reduced (Figure S21C). We further evaluated model performance with these calibrated parameters against multi-source datasets, and found that most simulated terrestrial and forest carbon fluxes and carbon pools are consistent with observation-based data (Note S1).

We also evaluated the model performance in forest age reconstruction according to an observation-based forest age map for 2010¹⁷ and forest inventory data¹⁶ (Figure 1). Forest inventory data refer to the statistical data published by China's forestry department,¹⁶ which is based on extensive field surveys. Gridded forest age map from Zhang et al.¹⁷ was generated by down-scaling the provincial statistics of national forest inventory data into 1-km resolution, which provides more detailed spatial information. Because of the discrepancy in the division of age groups in the forest inventory (1–27, 28–45, 46–65, 66–110, ≥111 years) and the model configuration (1–3, 4–9, 10–15, 16–30, 31–50, ≥51 years), for our comparison, we converted the six age cohorts to three age groups (1–27, 28–50, ≥51 years).

To test whether the model can capture the effects of elevated CO₂ on NPP, we ran four additional site simulations to compare with measurements from Free-Air CO₂ Enrichment (FACE) experiments.⁷⁵ These simulations were driven by fixed atmospheric CO₂ concentrations at 376 ppm or 550 ppm and varying climate forcing data to ensure consistency with the design of the FACE experiments. We chose the plant functional type (PFT) corresponding to the tree species at the FACE sites for comparison (Figure S18). We also used the annual mean NPP from S_{ref} and S_{CO_2} to test the sensitivity of NPP to elevated CO₂ against synthesized experiment-based results⁷⁶ and found that the simulated values are generally within the range of synthesis (Table S6).

In the model, after deforestation, a prescribed fraction of AGB is lost instantly to the atmosphere, and the remaining part goes to the litter pool. This prescribed fraction depends on the land-use types converted from forest (Table S5). In contrast, for forestry wood harvest, a fraction of AGB goes into the 10- and 100-year turnover wood product pools, with the fraction being forest-type specific (Table S5). The remaining biomass also goes into the litter pool. All the dead below-ground biomass carbon after deforestation and wood harvest will transfer to the litter pools.³⁴ Soil carbon will be inherited by the targeted youngest PFT after LUC and wood harvest using a weighted average method.³⁴ For example, after LUC from forest to cropland, soil carbon in the deforestation area will be removed from the forest soil carbon pool and merged to cropland soil carbon pool. Although carbon emissions from litter and soil decomposition have already been taken into account when calculating terrestrial NBP, the delayed carbon emissions from wood product pools are not included in NBP but analyzed separately (discussion and conclusions). It should be noted that wood products are temporary carbon storage pools, and the stored carbon will eventually be released into the atmosphere after the end of wood product life cycle.

Simulation setup

Five simulation stages were conducted using the calibrated ORCHIDEE-MICT at a half-degree resolution: spin-up, three historical periods (1700–1900, 1901–1959, and 1960–2019) and a series of future scenarios until 2100 (Figure S23). The spin-up simulations used a fixed atmospheric CO₂ concentration (the value in 1700)⁹³ and 6-hourly climate forcing data from the period 1901–1920 from CRUJRA, recycled as necessary,⁹⁴ and were run until the ecosystem carbon pools reached equilibrium. The same climate data were used to simulate the period between 1700 and 1900. To simulate F_{LULCC} during the period 1700–2019, we ran two sets of simulations with (S3) and without (S2) LULCC following the TRENDY project configuration.²⁶ The S2 simulation was driven by varying atmospheric CO₂ concentrations and using climate forcing data from CRUJRA but with a PFT map fixed at year 1700 values, while the S3 simulations were forced additionally by annual LUC and wood harvest. F_{LULCC} is calculated as the NBP difference between S3 and S2. For the S3 simulations for the period 1960–2019, we performed three simulations using different LULCC forcing data (Figure S23): (1) the default LUC maps (S_{def}) based on the Land-Use Harmonization (LUH2) data⁴⁴ as used for the global carbon budget in the TRENDY project,²⁶ (2) the area-adjusted LUC maps based on multiple remote sensing and inventory data, and national wood harvest data from Houghton & Nassikas⁴⁰ (S_{area}), and (3) the LUC maps and wood harvest data based on S_{area} but further constrained by gridded forest age maps¹⁷ (S_{age}). In the model, forests will be re-planted after wood harvest. The starting age cohort and the cohort sequence for wood harvest can be prescribed in the model. Following the LULCC history, the wood harvest during 1700–1979 was set to start at the oldest cohort and move to the progressively younger ones until the required harvest fraction was satisfied in each grid cell. After 1979, when most forest protection policies and ecological restoration programs began to be implemented, the wood harvest sequence in the model was changed to an order of 10~15, 16–30, 31–50, ≥51, 4–9, and 1–3. The starting age cohort (10–15 years) is generally in line with the rotation cycle of forest management in China,^{95,96} and the primary and old forests are largely reserved to be consistent with the forest conservation policies.⁹⁷

For the future period of 2020–2100, we designed a set of simulations to separate the effects of CO₂ increase, climate change, and new forest increase (Figure S23), consisting of (1) a reference simulation (S_{ref}) with climate conditions and atmospheric CO₂ concentrations and forest distribution all fixed at 2020 values, (2) simulations (S_{CO_2}) with time-variant CO₂ in addition to S_{ref} , (3) simulations (S_{clim}) also with varying climate conditions on top of S_{CO_2} , and (4) simulations (S_{newF}) with additional new forest increase based on the two methods of converting marginal croplands to forests. Therefore, the contribution of age-related growth in the existing forests can be derived from S_{ref} , and the contributions of CO₂ increase, climate change, and new forest increase after 2020 can be determined as the differences between S_{ref} and S_{CO_2} , S_{CO_2} and S_{clim} , and S_{clim} and S_{newF} , respectively. Note that climate change in this study refers to all changes in the climatic variables such as air temperature, precipitation, and downward longwave radiation; we did not further distinguish the contribution of each individual climatic factor. Future climate change and rising atmospheric CO₂ concentrations under RCP 2.6,

RCP 4.5, RCP 6.0, and RCP 8.5 were considered to represent four plausible future scenarios,⁹⁸ and the future climate forcing data were derived from the bias-corrected data of IPSL-CM5A-LR in the ISIMIP2b project.⁹⁹ A sensitivity test, regarding increased forest distribution, allowed us to investigate the response of position selection schemes for future afforestation projects to volatile climate change scenarios.

SUPPLEMENTAL INFORMATION

Supplemental information can be found online at <https://doi.org/10.1016/j.oneear.2024.04.011>.

ACKNOWLEDGMENTS

This study was supported by the National Natural Science Foundation of China (grant number: 72348001, 42175169 to W.L.; 42171096 to X.W.), the Yunnan Provincial Science and Technology Project at Southwest United Graduate School (grant number: 202302AO370001 to W.L.), the Hainan Institute of National Park grant (grant number: KY-23ZK01 to W.L.), the National Key R&D Program of China (grant number: 2019YFA0606604 to W.L.), and the Tsinghua University Initiative Scientific Research Program (grant number: 20223080041 to W.L.). The authors thank Richard A. Houghton for providing the updated wood harvest data.

AUTHOR CONTRIBUTIONS

Y.L., W.L., and P.C. designed the research; Y.L. and L.Z. performed the simulations; Y.L. performed the analysis; Y.L. and W.L. wrote the draft; and M.S., C.Y., J.C., Y.Y., Y.Z., J.Z., Z.L., X.W., Y.X., and S.P. contributed to the interpretation of the results and writing of the paper.

DECLARATION OF INTERESTS

The authors declare no competing interests.

Received: June 15, 2023

Revised: January 24, 2024

Accepted: April 22, 2024

Published: May 17, 2024

REFERENCES

- Pan, Y., Birdsey, R.A., Fang, J., Houghton, R., Kauppi, P.E., Kurz, W.A., Phillips, O.L., Shvidenko, A., Lewis, S.L., Canadell, J.G., et al. (2011). A large and persistent carbon sink in the world's forests. *Science* 333, 988–993. <https://doi.org/10.1126/science.1201609>.
- Dixon, R.K., Solomon, A.M., Brown, S., Houghton, R.A., Trexler, M.C., and Wisniewski, J. (1994). Carbon pools and flux of global forest ecosystems. *Science* 263, 185–190. <https://doi.org/10.1126/science.263.5144.185>.
- Bonan, G.B. (2008). Forests and climate change: Forcings, feedbacks, and the climate benefits of forests. *Science* 320, 1444–1449. <https://doi.org/10.1126/science.1155121>.
- Grassi, G., House, J., Dentener, F., Federici, S., den Elzen, M., and Penman, J. (2017). The key role of forests in meeting climate targets requires science for credible mitigation. *Nat. Clim. Change* 7, 220–226. <https://doi.org/10.1038/nclimate3227>.
- Pugh, T.A.M., Lindeskog, M., Smith, B., Poulter, B., Arnett, A., Haverd, V., and Calle, L. (2019). Role of forest regrowth in global carbon sink dynamics. *Proc. Natl. Acad. Sci. USA* 116, 4382–4387. <https://doi.org/10.1073/pnas.1810512116>.
- Chen, J.M. (2010). Modeling Long-term Forest Carbon Spatiotemporal Dynamics with Historical Climate and Recent Remote Sensing Data. *Sci. Found. China* 18, 38–79. <https://doi.org/10.1088/1005-0841/18/1/004>.
- Walker, A.P., De Kauwe, M.G., Bastos, A., Belmecheri, S., Georgiou, K., Keeling, R.F., McMahon, S.M., Medlyn, B.E., Moore, D.J.P., Norby, R.J., et al. (2021). Integrating the evidence for a terrestrial carbon sink caused by increasing atmospheric CO₂. *New Phytol.* 229, 2413–2445. <https://doi.org/10.1111/nph.16866>.
- Luyssaert, S., Schulze, E.D., Börner, A., Knohl, A., Hessenmöller, D., Law, B.E., Ciais, P., and Grace, J. (2008). Old-growth forests as global carbon sinks. *Nature* 455, 213–215. <https://doi.org/10.1038/nature07276>.
- Keenan, T.F., Gray, J., Friedl, M.A., Toomey, M., Bohrer, G., Hollinger, D.Y., Munger, J.W., O'Keefe, J., Schmid, H.P., Wing, I.S., et al. (2014). Net carbon uptake has increased through warming-induced changes in temperate forest phenology. *Nat. Clim. Change* 4, 598–604. <https://doi.org/10.1038/nclimate2253>.
- Piao, S., Ciais, P., Friedlingstein, P., Peylin, P., Reichstein, M., Luyssaert, S., Margolis, H., Fang, J., Barr, A., Chen, A., et al. (2008). Net carbon dioxide losses of northern ecosystems in response to autumn warming. *Nature* 451, 49–52. <https://doi.org/10.1038/nature06444>.
- Buermann, W., Forkel, M., O'Sullivan, M., Sitch, S., Friedlingstein, P., Haverd, V., Jain, A.K., Kato, E., Kautz, M., Lienert, S., et al. (2018). Widespread seasonal compensation effects of spring warming on northern plant productivity. *Nature* 562, 110–115. <https://doi.org/10.1038/s41586-018-0555-7>.
- Yu, Z., Ciais, P., Piao, S., Houghton, R.A., Lu, C., Tian, H., Agathokleous, E., Kattel, G.R., Sitch, S., Goll, D., et al. (2022). Forest expansion dominates China's land carbon sink since 1980. *Nat. Commun.* 13, 5374. <https://doi.org/10.1038/s41467-022-32961-2>.
- Fang, J., Guo, Z., Hu, H., Kato, T., Muraoka, H., and Son, Y. (2014). Forest biomass carbon sinks in East Asia, with special reference to the relative contributions of forest expansion and forest growth. *Global Change Biol.* 20, 2019–2030. <https://doi.org/10.1111/gcb.12512>.
- Tong, X., Brandt, M., Yue, Y., Ciais, P., Rudbeck Jepsen, M., Penuelas, J., Wigneron, J.P., Xiao, X., Song, X.P., Horion, S., et al. (2020). Forest management in southern China generates short term extensive carbon sequestration. *Nat. Commun.* 11, 129. <https://doi.org/10.1038/s41467-019-13798-8>.
- Lu, F., Hu, H., Sun, W., Zhu, J., Liu, G., Zhou, W., Zhang, Q., Shi, P., Liu, X., Wu, X., et al. (2018). Effects of national ecological restoration projects on carbon sequestration in China from 2001 to 2010. *Proc. Natl. Acad. Sci. USA* 115, 4039–4044. <https://doi.org/10.1073/pnas.1700294115>.
- National Forestry and Grassland Administration of the People's Republic of China (2019). *Ninth National Forest Resource Inventory Report (2014–2018)* (China Forestry Publishing House).
- Zhang, Y., Yao, Y., Wang, X., Liu, Y., and Piao, S. (2017). Mapping spatial distribution of forest age in China. *Earth Space Sci.* 4, 108–116. <https://doi.org/10.1002/2016ea000177>.
- Besnard, S., Koirala, S., Santoro, M., Weber, U., Nelson, J., Gütter, J., Haurault, B., Kass, J., N'Guessan, A., Neigh, C., et al. (2021). Mapping global forest age from forest inventories, biomass and climate data. *Earth Syst. Sci. Data* 13, 4881–4896. <https://doi.org/10.5194/essd-13-4881-2021>.
- Poorter, L., Bongers, F., Aide, T.M., Almeyda Zambrano, A.M., Balvanera, P., Becknell, J.M., Boukili, V., Brancalion, P.H.S., Broadbent, E.N., Chazdon, R.L., et al. (2016). Biomass resilience of Neotropical secondary forests. *Nature* 530, 211–214. <https://doi.org/10.1038/nature16512>.
- Tang, J., Luyssaert, S., Richardson, A.D., Kutsch, W., and Janssens, I.A. (2014). Steeper declines in forest photosynthesis than respiration explain age-driven decreases in forest growth. *Proc. Natl. Acad. Sci. USA* 111, 8856–8860. <https://doi.org/10.1073/pnas.1320761111>.
- Fang, J., Chen, A., Peng, C., Zhao, S., and Ci, L. (2001). Changes in forest biomass carbon storage in China between 1949 and 1998. *Science* 292, 2320–2322. <https://doi.org/10.1126/science.1058629>.
- Fang, J., Yu, G., Liu, L., Hu, S., and Chapin, F.S. (2018). Climate change, human impacts, and carbon sequestration in China INTRODUCTION. *Proc. Natl. Acad. Sci. USA* 115, 4015–4020. <https://doi.org/10.1073/pnas.1700304115>.
- Yu, G., Chen, Z., Piao, S., Peng, C., Ciais, P., Wang, Q., Li, X., and Zhu, X. (2014). High carbon dioxide uptake by subtropical forest ecosystems in

- the East Asian monsoon region. *Proc. Natl. Acad. Sci. USA* *111*, 4910–4915. <https://doi.org/10.1073/pnas.1317065111>.
24. Yao, Y., Li, Z., Wang, T., Chen, A., Wang, X., Du, M., Jia, G., Li, Y., Li, H., Luo, W., et al. (2018). A new estimation of China's net ecosystem productivity based on eddy covariance measurements and a model tree ensemble approach. *Agric. For. Meteorol.* *253–254*, 84–93. <https://doi.org/10.1016/j.agrformet.2018.02.007>.
 25. Piao, S., Fang, J., Ciais, P., Peylin, P., Huang, Y., Sitch, S., and Wang, T. (2009). The carbon balance of terrestrial ecosystems in China. *Nature* *458*, 1009–1013. <https://doi.org/10.1038/nature07944>.
 26. Friedlingstein, P., O'Sullivan, M., Jones, M.W., Andrew, R.M., Hauck, J., Olsen, A., Peters, G.P., Peters, W., Pongratz, J., Sitch, S., et al. (2020). Global Carbon Budget 2020. *Earth Syst. Sci. Data* *12*, 3269–3340. <https://doi.org/10.5194/essd-12-3269-2020>.
 27. He, H., Wang, S., Zhang, L., Wang, J., Ren, X., Zhou, L., Piao, S., Yan, H., Ju, W., Gu, F., et al. (2019). Altered trends in carbon uptake in China's terrestrial ecosystems under the enhanced summer monsoon and warming hiatus. *Natl. Sci. Rev.* *6*, 505–514. <https://doi.org/10.1093/nsr/nwz021>.
 28. Wang, J., Feng, L., Palmer, P.I., Liu, Y., Fang, S., Bösch, H., O'Dell, C.W., Tang, X., Yang, D., Liu, L., and Xia, C. (2020). Large Chinese land carbon sink estimated from atmospheric carbon dioxide data. *Nature* *586*, 720–723. <https://doi.org/10.1038/s41586-020-2849-9>.
 29. Wang, Y., Wang, X., Wang, K., Chevallier, F., Zhu, D., Lian, J., He, Y., Tian, H., Li, J., Zhu, J., et al. (2022). The size of the land carbon sink in China. *Nature* *603*, E7–E9. <https://doi.org/10.1038/s41586-021-04255-y>.
 30. Huang, B., Lu, F., Wang, X., Wu, X., Zhang, L., and Ouyang, Z. (2022). Ecological restoration and rising CO₂ enhance the carbon sink, counteracting climate change in northeastern China. *Environ. Res. Lett.* *17*, 014002. <https://doi.org/10.1088/1748-9326/ac3871>.
 31. Wang, S., Zhou, L., Chen, J., Ju, W., Feng, X., and Wu, W. (2011). Relationships between net primary productivity and stand age for several forest types and their influence on China's carbon balance. *J. Environ. Manag.* *92*, 1651–1662. <https://doi.org/10.1016/j.jenvman.2011.01.024>.
 32. Wang, B., Li, M., Fan, W., Yu, Y., and Chen, J. (2018). Relationship between Net Primary Productivity and Forest Stand Age under Different Site Conditions and Its Implications for Regional Carbon Cycle Study. *Forests* *9*, 5. <https://doi.org/10.3390/f9010005>.
 33. Fisher, J.B., Huntzinger, D.N., Schwalm, C.R., and Sitch, S. (2014). Modeling the Terrestrial Biosphere. *Annu. Rev. Environ. Resour.* *39*, 91–123. <https://doi.org/10.1146/annurev-environ-012913-093456>.
 34. Yue, C., Ciais, P., Luyssaert, S., Li, W., McGrath, M.J., Chang, J., and Peng, S. (2018). Representing anthropogenic gross land use change, wood harvest, and forest age dynamics in a global vegetation model ORCHIDEE-MICT v8.4.2. *Geosci. Model Dev.* *11*, 409–428. <https://doi.org/10.5194/gmd-11-409-2018>.
 35. National Bureau of Statistics of China (2021). *China Statistical Yearbook 2021* (China Statistics Press).
 36. Yang, Y., Shi, Y., Sun, W., Chang, J., Zhu, J., Chen, L., Wang, X., Guo, Y., Zhang, H., Yu, L., et al. (2022). Terrestrial carbon sinks in China and around the world and their contribution to carbon neutrality. *Sci. China Life Sci.* *65*, 861–895. <https://doi.org/10.1007/s11427-021-2045-5>.
 37. Guimberteau, M., Zhu, D., Maignan, F., Huang, Y., Yue, C., Dantec-Nédélec, S., Ottlé, C., Jornet-Puig, A., Bastos, A., Laurent, P., et al. (2018). ORCHIDEE-MICT (v8.4.1), a land surface model for the high latitudes: model description and validation. *Geosci. Model Dev. (GMD)* *11*, 121–163. <https://doi.org/10.5194/gmd-11-121-2018>.
 38. Liu, J., Kuang, W., Zhang, Z., Xu, X., Qin, Y., Ning, J., Zhou, W., Zhang, S., Li, R., Yan, C., et al. (2014). Spatiotemporal characteristics, patterns, and causes of land-use changes in China since the late 1980s. *J. Geogr. Sci.* *24*, 195–210. <https://doi.org/10.1007/s11442-014-1082-6>.
 39. He, F., Ge, Q., Dai, J., and Rao, Y. (2008). Forest change of China in recent 300 years. *J. Geogr. Sci.* *18*, 59–72. <https://doi.org/10.1007/s11442-008-0059-8>.
 40. Houghton, R.A., and Nassikas, A.A. (2017). Global and regional fluxes of carbon from land use and land cover change 1850–2015. *Global Biogeochem. Cycles* *31*, 456–472. <https://doi.org/10.1002/2016gb005546>.
 41. Food and Agriculture Organization of the United Nations (2020). *Global Forest Resources Assessment 2020: Main Report* (Food and Agriculture Organization of the United Nations).
 42. Klein Goldewijk, K., Beusen, A., Doelman, J., and Stehfest, E. (2017). Anthropogenic land use estimates for the Holocene - HYDE 3.2. *Earth Syst. Sci. Data* *9*, 927–953. <https://doi.org/10.5194/essd-9-927-2017>.
 43. China updated NDC (2021). Climate Action Tracker. <https://climateactiontracker.org/climate-target-update-tracker/china/>.
 44. Hurtt, G.C., Chini, L., Sahajpal, R., Frolking, S., Bodirsky, B.L., Calvin, K., Doelman, J.C., Fisk, J., Fujimori, S., Klein Goldewijk, K., et al. (2020). Harmonization of global land use change and management for the period 850–2100 (LUH2) for CMIP6. *Geosci. Model Dev. (GMD)* *13*, 5425–5464. <https://doi.org/10.5194/gmd-13-5425-2020>.
 45. Chang, J., Ciais, P., Wang, X., Piao, S., Asrar, G., Betts, R., Chevallier, F., Dury, M., François, L., Frieler, K., et al. (2017). Benchmarking carbon fluxes of the ISIMIP2a biome models. *Environ. Res. Lett.* *12*, 045002. <https://doi.org/10.1088/1748-9326/aa63fa>.
 46. Hansis, E., Davis, S.J., and Pongratz, J. (2015). Relevance of methodological choices for accounting of land use change carbon fluxes. *Global Biogeochem. Cycles* *29*, 1230–1246. <https://doi.org/10.1002/2014gb004997>.
 47. Campbell, J.E., Lobell, D.B., Genova, R.C., and Field, C.B. (2008). The global potential of bioenergy on abandoned agriculture lands. *Environ. Sci. Technol.* *42*, 5791–5794. <https://doi.org/10.1021/es800052w>.
 48. Piao, S., He, Y., Wang, X., and Chen, F. (2022). Estimation of China's terrestrial ecosystem carbon sink: Methods, progress and prospects. *Sci. China Earth Sci.* *65*, 641–651. <https://doi.org/10.1007/s11430-021-9892-6>.
 49. Zhao, W., Tan, W., and Li, S. (2021). High leaf area index inhibits net primary production in global temperate forest ecosystems. *Environ. Sci. Pollut. Res. Int.* *28*, 22602–22611. <https://doi.org/10.1007/s11356-020-11928-0>.
 50. Shang, R., Chen, J.M., Xu, M., Lin, X., Li, P., Yu, G., He, N., Xu, L., Gong, P., Liu, L., et al. (2023). China's current forest age structure will lead to weakened carbon sinks in the near future. *Innovation* *4*, 100515. <https://doi.org/10.1016/j.xinn.2023.100515>.
 51. Powers, M.D., Kolka, R.K., Bradford, J.B., Palik, B.J., Fraver, S., and Jurgensen, M.F. (2012). Carbon stocks across a chronosequence of thinned and unmanaged red pine (*Pinus resinosa*) stands. *Ecol. Appl.* *22*, 1297–1307. <https://doi.org/10.1890/11-0411.1>.
 52. Dang, X., Liu, G., Zhao, L., and Zhao, G. (2017). The response of carbon storage to the age of three forest plantations in the Loess Hilly Regions of China. *Catena* *159*, 106–114. <https://doi.org/10.1016/j.catena.2017.08.013>.
 53. He, N., Wen, D., Zhu, J., Tang, X., Xu, L., Zhang, L., Hu, H., Huang, M., and Yu, G. (2017). Vegetation carbon sequestration in Chinese forests from 2010 to 2050. *Global Change Biol.* *23*, 1575–1584. <https://doi.org/10.1111/gcb.13479>.
 54. Yao, Y., Piao, S., and Wang, T. (2018). Future biomass carbon sequestration capacity of Chinese forests. *Sci. Bull.* *63*, 1108–1117. <https://doi.org/10.1016/j.scib.2018.07.015>.
 55. Zhu, Z., Piao, S., Myneni, R.B., Huang, M., Zeng, Z., Canadell, J.G., Ciais, P., Sitch, S., Friedlingstein, P., Arneeth, A., et al. (2016). Greening of the Earth and its drivers. *Nat. Clim. Change* *6*, 791–795. <https://doi.org/10.1038/nclimate3004>.
 56. Hong, S., Yin, G., Piao, S., Dybzinski, R., Cong, N., Li, X., Wang, K., Peñuelas, J., Zeng, H., and Chen, A. (2020). Divergent responses of soil organic carbon to afforestation. *Nat. Sustain.* *3*, 694–700. <https://doi.org/10.1038/s41893-020-0557-y>.
 57. Hou, G., Delang, C.O., Lu, X., and Gao, L. (2020). A meta-analysis of changes in soil organic carbon stocks after afforestation with deciduous

- broadleaved, sempervirent broadleaved, and conifer tree species. *Ann. For. Sci.* 77, 92. <https://doi.org/10.1007/s13595-020-00997-3>.
58. Lu, N., Tian, H., Fu, B., Yu, H., Piao, S., Chen, S., Li, Y., Li, X., Wang, M., Li, Z., et al. (2022). Biophysical and economic constraints on China's natural climate solutions. *Nat. Clim. Change* 12, 847–853. <https://doi.org/10.1038/s41558-022-01432-3>.
 59. Zhang, D., Zuo, X., and Zang, C. (2021). Assessment of future potential carbon sequestration and water consumption in the construction area of the Three-North Shelterbelt Programme in China. *Agric. For. Meteorol.* 303, 108377. <https://doi.org/10.1016/j.agrformet.2021.108377>.
 60. Xu, L., Zheng, C., and Ma, Y. (2021). Variations in precipitation extremes in the arid and semi-arid regions of China. *Int. J. Climatol.* 41, 1542–1554. <https://doi.org/10.1002/joc.6884>.
 61. Feng, D., Fu, M., Sun, Y., Bao, W., Zhang, M., Zhang, Y., and Wu, J. (2021). How Large-Scale Anthropogenic Activities Influence Vegetation Cover Change in China? A Review. *Forests* 12, 320. <https://doi.org/10.3390/f12030320>.
 62. Veldman, J.W., Overbeck, G.E., Negreiros, D., Mahy, G., Le Stradic, S., Fernandes, G.W., Durigan, G., Buisson, E., Putz, F.E., and Bond, W.J. (2015). Where Tree Planting and Forest Expansion are Bad for Biodiversity and Ecosystem Services. *Bioscience* 65, 1011–1018. <https://doi.org/10.1093/biosci/biv118>.
 63. Hua, F., Buijnzeel, L.A., Meli, P., Martin, P.A., Zhang, J., Nakagawa, S., Miao, X., Wang, W., McEvoy, C., Peña-Arancibia, J.L., et al. (2022). The biodiversity and ecosystem service contributions and trade-offs of forest restoration approaches. *Science* 376, 839–844. <https://doi.org/10.1126/science.abl4649>.
 64. Xu, H., Yue, C., Zhang, Y., Liu, D., and Piao, S. (2023). Forestation at the right time with the right species can generate persistent carbon benefits in China. *Proc. Natl. Acad. Sci. USA* 120, e2304988120. <https://doi.org/10.1073/pnas.2304988120>.
 65. Yu, Z., You, W., Agathokleous, E., Zhou, G., and Liu, S. (2021). Forest management required for consistent carbon sink in China's forest plantations. *For. Ecosyst.* 8, 54. <https://doi.org/10.1186/s40663-021-00335-7>.
 66. Schädler, C., Bader, M.K.F., Schuur, E.A.G., Biasi, C., Bracho, R., Čapek, P., De Baets, S., Diáková, K., Ernakovich, J., Estop-Aragones, C., et al. (2016). Potential carbon emissions dominated by carbon dioxide from thawed permafrost soils. *Nat. Clim. Change* 6, 950–953. <https://doi.org/10.1038/nclimate3054>.
 67. Duan, H., Zhou, S., Jiang, K., Bertram, C., Harmsen, M., Krieglner, E., van Vuuren, D.P., Wang, S., Fujimori, S., Tavoni, M., et al. (2021). Assessing China's efforts to pursue the 1.5 degrees C warming limit. *Science* 372, 378–385. <https://doi.org/10.1126/science.aba8767>.
 68. Yue, C., Ciais, P., and Li, W. (2018). Smaller global and regional carbon emissions from gross land use change when considering sub-grid secondary land cohorts in a global dynamic vegetation model. *Biogeosciences* 15, 1185–1201. <https://doi.org/10.5194/bg-15-1185-2018>.
 69. Churkina, G., Organschi, A., Reyer, C.P.O., Ruff, A., Vinke, K., Liu, Z., Reck, B.K., Graedel, T.E., and Schellnhuber, H.J. (2020). Buildings as a global carbon sink. *Nat. Sustain.* 3, 269–276. <https://doi.org/10.1038/s41893-019-0462-4>.
 70. Mishra, A., Humpenöder, F., Churkina, G., Reyer, C.P.O., Beier, F., Bodirsky, B.L., Schellnhuber, H.J., Lotze-Campen, H., and Popp, A. (2022). Land use change and carbon emissions of a transformation to timber cities. *Nat. Commun.* 13, 4889. <https://doi.org/10.1038/s41467-022-32244-w>.
 71. Pregitzer, K.S., and Euskirchen, E.S. (2004). Carbon cycling and storage in world forests: biome patterns related to forest age. *Global Change Biol.* 10, 2052–2077. <https://doi.org/10.1111/j.1365-2486.2004.00866.x>.
 72. Allen, C.D., Macalady, A.K., Chenchouni, H., Bachelet, D., McDowell, N., Vennetier, M., Kitzberger, T., Rigling, A., Breshears, D.D., Hogg, E.T., et al. (2010). A global overview of drought and heat-induced tree mortality reveals emerging climate change risks for forests. *For. Ecol. Manage.* 259, 660–684. <https://doi.org/10.1016/j.foreco.2009.09.001>.
 73. Choat, B., Brodribb, T.J., Brodersen, C.R., Duursma, R.A., López, R., and Medlyn, B.E. (2018). Triggers of tree mortality under drought. *Nature* 558, 531–539. <https://doi.org/10.1038/s41586-018-0240-x>.
 74. Bottero, A., Garbarino, M., Long, J.N., and Motta, R. (2013). The interacting ecological effects of large-scale disturbances and salvage logging on montane spruce forest regeneration in the western European Alps. *For. Ecol. Manage.* 292, 19–28. <https://doi.org/10.1016/j.foreco.2012.12.021>.
 75. Norby, R.J., DeLucia, E.H., Gielen, B., Calfapietra, C., Giardina, C.P., King, J.S., Ledford, J., McCarthy, H.R., Moore, D.J.P., Ceulemans, R., et al. (2005). Forest response to elevated CO₂ is conserved across a broad range of productivity. *Proc. Natl. Acad. Sci. USA* 102, 18052–18056. <https://doi.org/10.1073/pnas.0509478102>.
 76. Song, J., Wan, S., Piao, S., Knapp, A.K., Classen, A.T., Vicca, S., Ciais, P., Hovenden, M.J., Leuzinger, S., Beier, C., et al. (2019). A meta-analysis of 1,119 manipulative experiments on terrestrial carbon-cycling responses to global change. *Nat. Ecol. Evol.* 3, 1309–1320. <https://doi.org/10.1038/s41559-019-0958-3>.
 77. Wu, Z., Huang, X., Chen, R., Mao, X., and Qi, X. (2022). The United States and China on the paths and policies to carbon neutrality. *J. Environ. Manag.* 320, 115785. <https://doi.org/10.1016/j.jenvman.2022.115785>.
 78. Cai, W., Wang, G., Santoso, A., McPhaden, M.J., Wu, L., Jin, F.F., Timmermann, A., Collins, M., Vecchi, G., Lengaigne, M., et al. (2015). Increased frequency of extreme La Nina events under greenhouse warming. *Nat. Clim. Change* 5, 132–137. <https://doi.org/10.1038/nclimate2492>.
 79. Dai, L., Li, S., Zhou, W., Qi, L., Zhou, L., Wei, Y., Li, J., Shao, G., and Yu, D. (2018). Opportunities and challenges for the protection and ecological functions promotion of natural forests in China. *For. Ecol. Manage.* 410, 187–192. <https://doi.org/10.1016/j.foreco.2017.09.044>.
 80. Houghton, R.A., Byers, B., and Nassikas, A.A. (2015). COMMENTARY: A role for tropical forests in stabilizing atmospheric CO₂. *Nat. Clim. Change* 5, 1022–1023. <https://doi.org/10.1038/nclimate2869>.
 81. Winkler, K., Fuchs, R., Rounsevell, M., and Herold, M. (2021). Global land use changes are four times greater than previously estimated. *Nat. Commun.* 12, 2501. <https://doi.org/10.1038/s41467-021-22702-2>.
 82. Messier, C., Bauhus, J., Doyon, F., Maure, F., Sousa-Silva, R., Nolet, P., Mina, M., Aquilué, N., Fortin, M.J., and Puettmann, K. (2019). The functional complex network approach to foster forest resilience to global changes. *For. Ecosyst.* 6, 21. <https://doi.org/10.1186/s40663-019-0166-2>.
 83. Riviere, M., and Cauria, S. (2021). Landscape implications of managing forests for carbon sequestration. *Forestry* 94, 70–85. <https://doi.org/10.1093/forestry/cpaa015>.
 84. Martes, L., and Köhl, M. (2022). Improving the Contribution of Forests to Carbon Neutrality under Different Policies-A Case Study from the Hamburg Metropolitan Area. *Sustainability* 14, 2088. <https://doi.org/10.3390/su14042088>.
 85. Zickfeld, K., Macisaac, A.J., Canadell, J.G., Fuss, S., Jackson, R.B., Jones, C.D., Lohila, A., Matthews, H.D., Peters, G.P., Rogelj, J., and Zaehle, S. (2023). Net-zero approaches must consider Earth system impacts to achieve climate goals. *Nat. Clim. Change* 13, 1298–1305. <https://doi.org/10.1038/s41558-023-01862-7>.
 86. Li, Y., Piao, S., Li, L.Z.X., Chen, A., Wang, X., Ciais, P., Huang, L., Lian, X., Peng, S., Zeng, Z., et al. (2018). Divergent hydrological response to large-scale afforestation and vegetation greening in China. *Sci. Adv.* 4, eaar4182. <https://doi.org/10.1126/sciadv.aar4182>.
 87. Fang, J.Y., Guo, Z.D., Piao, S.L., and Chen, A.P. (2007). Estimation of terrestrial vegetation carbon sinks in China from 1981 to 2000. *Sci. China Earth Sci.* 37, 804–812.
 88. Peng, S., Ciais, P., Maignan, F., Li, W., Chang, J., Wang, T., and Yue, C. (2017). Sensitivity of land use change emission estimates to historical land use and land cover mapping. *Global Biogeochem. Cycles* 31, 626–643. <https://doi.org/10.1002/2015gb005360>.
 89. Zhou, T., Shi, P., Jia, G., Dai, Y., Zhao, X., Shangguan, W., Du, L., Wu, H., and Luo, Y. (2015). Age-dependent forest carbon sink: Estimation via

- inverse modeling. *JGR. Biogeosciences* 120, 2473–2492. <https://doi.org/10.1002/2015JG002943>.
90. Krinner, G., Viovy, N., de Noblet-Ducoudré, N., Ogée, J., Polcher, J., Friedlingstein, P., Ciais, P., Sitch, S., and Prentice, I.C. (2005). A dynamic global vegetation model for studies of the coupled atmosphere-biosphere system. *Global Biogeochem. Cycles* 19, Gb1015. <https://doi.org/10.1029/2003gb002199>.
91. Yue, C., Ciais, P., Houghton, R.A., and Nassikas, A.A. (2020). Contribution of land use to the interannual variability of the land carbon cycle. *Nat. Commun.* 11, 3170. <https://doi.org/10.1038/s41467-020-16953-8>.
92. Wang, Y.Q. (2017). *Remote Sensing Quantitative Inversion of Maximum Carboxylation Rate by Hyperspectral Data (Northeast Forestry University). (Masters Dissertation)*.
93. Dlugokencky, E., and Tans, P. (2020). Trends in atmospheric carbon dioxide. In *National Oceanic and Atmospheric Administration, and Earth System Research Laboratory (NOAA/ESRL)*.
94. University of East Anglia Climatic Research Unit, and Harris, I.C. (2021). CRU JRA v2.2: A forcings dataset of gridded land surface blend of Climatic Research Unit (CRU) and Japanese reanalysis (JRA) data; Jan.1901 - Dec.2020. In *NERC EDS Centre for Environmental Data Analysis*.
95. van Dijk, A.I., and Keenan, R.J. (2007). Planted forests and water in perspective. *For. Ecol. Manage.* 251, 1–9. <https://doi.org/10.1016/j.foreco.2007.06.010>.
96. Zhao, M., Xiang, W., Peng, C., and Tian, D. (2009). Simulating age-related changes in carbon storage and allocation in a Chinese fir plantation growing in southern China using the 3-PG model. *For. Ecol. Manage.* 257, 1520–1531. <https://doi.org/10.1016/j.foreco.2008.12.025>.
97. Fu, B., Liu, Y., and Meadows, M.E. (2023). Ecological restoration for sustainable development in China. *Natl. Sci. Rev.* 10, nwad033. <https://doi.org/10.1093/nsr/nwad033>.
98. van Vuuren, D.P., Edmonds, J., Kainuma, M., Riahi, K., Thomson, A., Hibbard, K., Hurtt, G.C., Kram, T., Krey, V., Lamarque, J.F., et al. (2011). The representative concentration pathways: an overview. *Clim. Change* 109, 5–31. <https://doi.org/10.1007/s10584-011-0148-z>.
99. Frieler, K., Lange, S., Piontek, F., Reyer, C.P.O., Schewe, J., Warszawski, L., Zhao, F., Chini, L., Denvil, S., Emanuel, K., et al. (2017). Assessing the impacts of 1.5 degrees C global warming - simulation protocol of the Inter-Sectoral Impact Model Intercomparison Project (ISIMIP2b). *Geosci. Model Dev. (GMD)* 10, 4321–4345. <https://doi.org/10.5194/gmd-10-4321-2017>.